

GCFR IRRADIATION EXPERIMENTS

This is a preprint of a paper to be presented at the International Conference on Fast Breeder Reactor Fuel Performance, March 5-8, 1979, Monterey, California, and to be published in the Proceedings.

**Work supported in part by
Department of Energy
Contract EY-76-C-03-0167, Project Agreement No. 23**

**GENERAL ATOMIC PROJECT 6113
OCTOBER 1978**

GENERAL ATOMIC COMPANY

DISCLAIMER

This report was prepared as an account of work sponsored by an agency of the United States Government. Neither the United States Government nor any agency thereof, nor any of their employees, makes any warranty, express or implied, or assumes any legal liability or responsibility for the accuracy, completeness, or usefulness of any information, apparatus, product, or process disclosed, or represents that its use would not infringe privately owned rights. Reference herein to any specific commercial product, process, or service by trade name, trademark, manufacturer, or otherwise does not necessarily constitute or imply its endorsement, recommendation, or favoring by the United States Government or any agency thereof. The views and opinions of authors expressed herein do not necessarily state or reflect those of the United States Government or any agency thereof.

DISCLAIMER

Portions of this document may be illegible in electronic image products. Images are produced from the best available original document.

CONTENTS

PART I. IRRADIATION EXPERIMENTS IN THE DEVELOPMENT OF A VENTED, HELIUM-COOLED FAST BREEDER REACTOR FUEL DESIGN

1.	INTRODUCTION	3
2.	RESULTS OF VENTED SWEEP GAS IRRADIATION EXPERIMENTS GB-9 AND GB-10	5
2.1.	Fission Gas Release from Vented Rods GB-9 and GB-10	5
2.1.1.	GB-9 Results	5
2.1.2.	GB-10 Results	8
3.	F-1 (X094) FAST FLUX IRRADIATION EXPERIMENT	11
3.1.	Burnups and Behavior of Sol-Gel Fuel in F-1 Fuel Rods	11
3.2.	Fission Gas Release from F-1 Fuel Rods	11
3.3.	Fuel Clad Chemical Interaction in F-1 Fuel Rods	14
3.4.	Dosimetry and Tritium Analyses for F-1 (X094) Experiment	15
4.	F-3 (X206) FAST FLUX EXPERIMENT	15
5.	DIAMETRICAL CHANGES IN GCFR FUEL RODS	15
5.1.	Diametral Changes in GCFR Vented Fuel Rods Irradiated in Thermal Flux	16
5.2.	Diametral Changes in Simulated Vented Rods in Fast Flux	16
5.3.	Diametral Changes in Ribbed Rods Compared to Smooth Rods	18
5.4.	Diametral Changes in GCFR Rods Compared to LMFBR Rods	23
6.	F-5 (X317) GRID-SPACED FUEL ROD BUNDLE EXPERIMENT IN EBR-II	23
6.1.	F-5 Description	23
6.2.	F-5 Status/Plans	24

7. HELM SERIES OF VENTED ROD BUNDLE IRRADIATIONS IN BR2 AT MOL	29
8. CONCLUSIONS	29
REFERENCES	30

FIGURES

1. Schematic of fuel element pressure equalization system (PES)	4
2. GCFR capsule GB-10 release (R/B) and venting (V/B) fractions	9
3. Fission gas release versus fuel rod burnup	12
4. Profilometry of diameter for rod G-8 at 0°, 90° and 45°, 135° orientations	16
5. Profilometry of diameter for rod G-4 at 0°, 90°, and 45°, 135° orientations	19
6. Profilometry of diameter for rod G-9 at 0°, 90° and 45°, 135° orientations	19
7. Profilometry of diameter for rod G-10 (ribbed cladding) at 0°, 90° and 45°, 135° orientations	20
8. Profilometry of diameter for rod G-11 (ribbed cladding) at 0°, 90° and 45°, 135° orientations	20
9. Profilometry of diameter for rod G-12 at 0°, 90° and 45°, 135° orientations	21
10. Profilometry of diameter for rod G-13 at 0°, 90° and 45°, 135° orientations	21
11. Plot of diametral increases versus maximum cladding temperature during irradiation for the F-1 (X094) fuel rods. Numbers in parentheses are exposure values in atom percent	22
12. GCFR F-5 fuel pin assembly	24
13. The F-5 (X317) grid-spaced bundle design	25
14. Summary of F-5 irradiation plan showing fuel rods	27
15. F-5 grid-spaced bundle skeleton after assembly	28
16. F-5 (X317) grid-spaced fuel rod bundle after final loading with cold-worked 316 SS clad, (Pu-U) ₂ fueled rods at EBR-II	28

TABLES

I.	Objectives of GCFR irradiation tests	4
II.	Design conditions and results/status for GCFR thermal flux and epithermal flux vented rod irradiation experiments in ORR [U.S. and BR2 (Europe)]	6
III.	Design conditions and results/status for GCFR fast flux irradiation experiments in EBR-II	7
IV.	Calculated R/Bs from V/Bs measured in capsule GB-9	8
V.	Irradiation conditions for F-1 (X094) fast flux irradiation experiment fuel rods	10
VI.	Fuel burnup analysis	12
VII.	Results of gas sampling and analyses for F-1 fuel rods	13
VIII.	Summary of profilometry results for F-1 rods in final portion of X094 irradiation	17
IX.	Profilometry data (condensed) for F-1	22
X.	Fuel rod design data	26
XI.	Fuel rod nomenclature denoting design variables	27
PART 2. IRRADIATION OF GCFR TEST FUEL BUNDLES IN THE BR2 HELIUM LOOP-MOL		
1.	INTRODUCTION	35
2.	COMPARISON WITH A DEMO PLANT	36
3.	CONSTRUCTION OF THE FUEL ELEMENT	36
3.1.	Fuel Element Bundle	36
3.2.	In-Pile Section	37
3.3.	Pressure Equalization System	37
4.	PRELIMINARY EXPERIMENTS	39
5.	RESULTS	41
5.1.	Tritium	41
5.2.	Iodine	42
6.	FUTURE EXPERIMENTAL WORK	42
	REFERENCES	42

FIGURE

1. Principle of pressure equalization system 38

TABLE

I. Comparison of loop and reactor parameters 36

**PART 1. IRRADIATION EXPERIMENTS IN THE
DEVELOPMENT OF A VENTED, HELIUM-COOLED FAST
BREEDER REACTOR FUEL DESIGN**

**J. R. LINDGREN, S. LANGER, R. J. CAMPANA
R. T. ACHARYA, P. W. FLYNN, and G. BUZZELLI
S. GREENBERG
Argonne National Laboratory, Argonne, Illinois
A. W. LONGEST, JR.
Oak Ridge National Laboratory, Oak Ridge, Tennessee**

PART. I. IRRADIATION EXPERIMENTS IN THE DEVELOPMENT OF A VENTED,
HELIUM-COOLED FAST BREEDER REACTOR FUEL DESIGN

1. INTRODUCTION

The fuel rods in the gas-cooled fast breeder reactor (GCFR) are vented and pressure equalized (see Fig. 1) to avoid creep collapse of the cladding under external overpressure of 9 MPa (90 atm) of the helium coolant. In other respects the fuel rod design and materials (20% cold-worked 316 stainless steel cladding, 25% Pu - 75% UO₂ fueled rods) are the same as those for the liquid metal fast breeder reactor (LMFBR). An irradiation program in the U.S., which is sponsored by DOE and has been a cooperative effort among General Atomic (GA), Argonne National Laboratory (ANL), and Oak Ridge National Laboratory (ORNL), is being conducted to verify the performance of the GCFR fuel rods. An additional experiment, consisting of a vented rod bundle test in BR2 at Mol, Belgium, is a cooperative effort among Kernforschungsanlage (KFA), Kraftwerk Union (KWU), Kernforschungszentrum Karlsruhe (KFK), and GA. The irradiations include thermal flux tests in ORR (U.S.), epithermal flux tests in BR2 (Europe), and fast flux tests in the Experimental Breeder Reactor II (EBR-II) which include single rod and multirod bundle experiments.

The GCFR thermal flux mixed oxide fuel rod tests consisted of sealed rod experiment P-8 and vented rod sweep gas capsule experiments GB-9¹ and GB-10² in ORR. The GCFR epithermal flux tests include planned single-rod vented sweep gas experiment GB-11 and the helium loop tests of 12-ribbed-rod, vented bundle tests HELM 2 (UO₂ fueled) and HELM 3 (PuO₂-UO₂ fueled), which are currently under way. The GCFR fast flux experiments consist of 13 encapsulated rods (7 rods at a time) in F-1 (X094)³, 10 encapsulated rods in F-3 (X206), and 43 unencapsulated rods (31 rods at a time) in the F-5 (X317) grid spaced bundle experiment⁴. The objectives of the GCFR irradiation tests are given in Table I.

The conditions and results/status for the thermal flux tests in ORR and the epithermal flux tests in BR2 are given in summary form in Table II. The conditions and results/status for the fast flux tests in EBR-II are given in Table III. The results of the tests to date show very satisfactory performance for both vented rods tested in the thermal flux and epithermal flux irradiations and for simulated vented (large plenum)

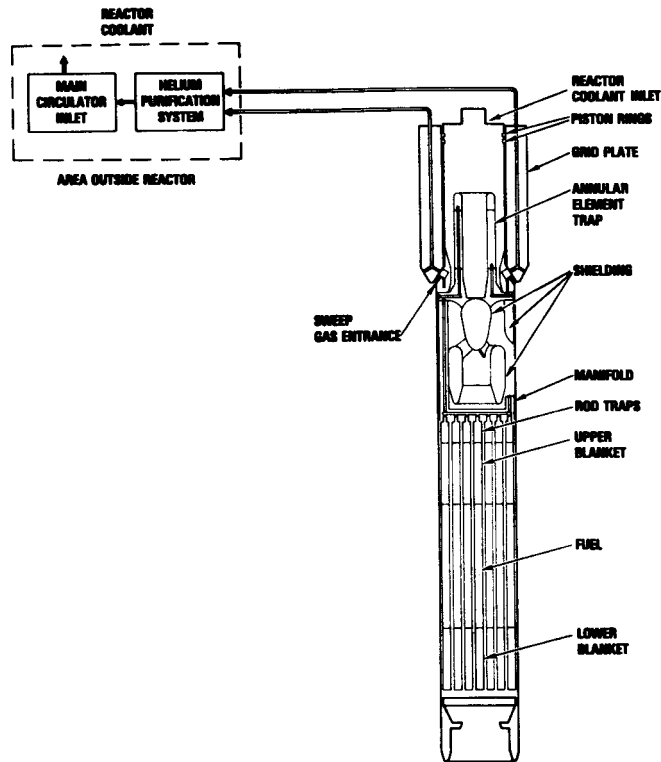


Fig. 1. Schematic of fuel element pressure equalization system (PES)

TABLE I. OBJECTIVES OF GCFR IRRADIATION TESTS

Major Objectives

- Verify performance models for GCFR conditions
- Verify applicability of LMFBR experience to GCFR design
- Verify applicability of GCFR thermal irradiation experience
- Measure ribbed cladding behavior
- Establish overtemperature margin
- Obtain fuel lifetime failure statistics (reliability)
- Determine failure mode for GCFR design
- Determine behavior associated with element rotation
(slow step power change)
- Measure fission product trap performance
- Verify operation of PES

Secondary Objectives

- Measure neutron shielding performance
- Measure thermocouple performance

rods tested in fast flux irradiations. The detailed results and status for the GCFR irradiations are discussed in the following sections.

2. RESULTS OF VENTED SWEEP GAS IRRADIATION EXPERIMENTS GB-9 AND GB-10

Among the objectives of the GB-9⁵ and GB-10 thermal flux irradiation experiments, the most important were to measure or determine the venting fraction of the radioactive fission gases, the release and transport of the volatile fission products (cesium and iodine), and the fuel fission product cladding chemical reactions. The peak burnup exposures for the fuel rods in these experiments were 5.84 at. % for GB-9 and 10.98 at. % for GB-10.

2.1. Fission Gas Release from Vented Rods GB-9 and GB-10

Fission gas release and venting were measured from the GCFR vented fuel rods irradiated in capsules GB-9 and GB-10. The release rate R is defined here as the rate at which gaseous fission products born in fission of the fuel are released from the solid-state matrix of the mixed oxide fuel into the gas phase of the interstices of the fuel region. The venting rate V , however, is defined as the rate at which the gaseous fission products are released and then transported in the gas phase from the fuel region through the blanket and trap regions to the fuel rod vent. Dividing the release and venting rates by the birth rate B then results in R/B and V/B , the release and venting fractions, respectively. There is usually little distinction between release and venting fractions, but in the GCFR, with high-pressure helium (86 atm) in the fuel rod, there is much greater impedance to the gas-phase transport, which results in significant differences in the R/B and V/B values.

2.1.1. GB-9 Results. With the plumbing of capsule GB-9, only V/B could be measured. Vial grab samples were taken from the effluent sweep gas stream and subsequently counted using a laboratory NaI (Tl) gamma spectrometer. To deduce the R/B values it was necessary to divide the measured V/B s by the calculated V/R s. The V/R s were calculated using SLIDER,⁶ a computer program which uses the finite-difference numerical method to solve the one-dimension gaseous diffusion transport equation including a radioactive decay term. Thus V/B s, V/R s, and R/B s are all functions of the isotope half-lives. The V/B s measured in GB-9 at steady-state conditions of 49 kW/m and 685°C cladding outer surface temperature after a burnup of 5.4 at. %, calculated V/R s, and deduced R/B s are given in Table IV.

TABLE II. DESIGN CONDITIONS AND RESULTS/STATUS FOR GCFR THERMAL FLUX AND EPITHERMAL FLUX VENTED ROD IRRADIATION EXPERIMENTS IN ORR [U.S. AND BR2 (EUROPE)]

	Linear Rating [W/cm (time)]	Cladding O.D. Temp (°C)	Burnup (at. %)	Trap Temp (°C)	Sweep Gas Pressure [MPa (psig)]	ΔP Across Cladding [MPa (psig)]	Cladding Surface	Fuel Pellet Geometry	Fuel O/M ^(a)	Release Measurement Capability	Results/Status
P-8: 3 sealed rods in ORR facility, thermal flux	400 to 500 (460 days)	610 to 700	6.5	NA	Static pressure, no sweep, 6.9 (1000)	Up to 6.9 (1000)	Smooth	Annular (90% TD)	1.98/ 1.99	NA	All fuel rods in excellent condition; little, if any, deformation observed
GB-9: sweep-gas capsule in ORR poolside facility, thermal flux	486 (471 days)	685	5.84	300	6.9 (1000)	0.17 (25)	Smooth	Annular (92% TD)	1.98	a. Top of rod b. Bottom of rod	No dimensional change. Fission gas release as expected based on calculations. No volatile fission product (Cs and I) transport beyond trap. Fuel fission product cladding attack same as for LMFBR rods
GB-10: sweep-gas capsule in ORR poolside facility, thermal flux	394 (295 days) 443 (498 days) 486 (179 days)	565 630 685	10.98	300	6.9 (1000)	0.17 (25)	Ribbed	Solid (88% TD)	1.97	a. Top of rod b. Bottom of rod c. Bottom of blanket d. Leak simulation	No dimensional change. Fission gas release as expected based on calculations. Minimal volatile fission product (Cs and I) transport beyond trap. Resistance to sweep gas flow increased with burnup. Fuel fission product cladding attack same as for LMFBR rods.
HELM II (UO ₂ -fueled) and HELM III [(Pu-U)O ₂ fueled]: 12-rod bundles in BR2 helium loop in cadmium-filtered epithermal flux	460	670	10.8 (goal for HELM III)	300	6.9 (1000)	0.17 (25)	Ribbed	Solid (88% TD)	1.945/ 1.975	a. Top of rod	Irradiation of UO ₂ -fueled bundle completed; irradiation of UO ₂ -PuO ₂ -fueled bundle initiated.

(a) O/M = oxygen/metal ratio.

TABLE III. DESIGN CONDITIONS AND RESULTS/STATUS FOR GCFR FAST FLUX IRRADIATION EXPERIMENTS IN EBR-II

	Linear Rating (W/cm)	Cladding I.D. Temp (°C)	Burnup (at. %)	Cladding Surface	Fuel Pellet Geometry	Fuel O/M	Results/Status
F-1 (X094): encapsulated rod test	420 to 504	648 to 759	2.7 to 13.6	11 smooth, 2 ribbed	Annular (92% TD) in 11 rods, solid (88% TD) in 2 rods	1.98 ± 0.01 except for G-9; 1.95	All rods intact. No more than 0.06 mm (0.0025 in.) attack after exposure up to 750°C. No difference in strain in ribbed rods vs smooth rods.
F-3 (X206): encapsulated rod test	453 to 535	676 to 749	5.0	Ribbed	Annular (92% TD) in 3 rods, solid (88% TD) in 7 rods	1.94 in 6 rods; 1.98 in 4 rods	Nine of 10 rods failed due to inadequate capsule sodium bond.
F-5 (X317): unencapsulated rod, grid spaced bundle test	368 to 404	700	10.8 (goal)	Ribbed	Solid (91% TD)	1.96 ± 0.01	Irradiation of initial 31 rod portion of experiment started 1/21/78.

TABLE IV. CALCULATED R/Bs FROM V/Bs MEASURED IN CAPSULE GB-9

Isotope	Half-Life	Measured V/B (%)	Calculated V/R (%)	R/B
Kr-85m	4.4 h	3.5	4.96	70.6
Kr-87	1.3 h	0.67	0.49	137.0
Kr-88	2.8 h	1.10	2.40	45.8
Xe-133	5.3 h	23.0	62.0	37.0
Xe-135m	15.7 m	1.8	10.5	17.1
Xe-135	9.2 h	0.015	10.0 ⁻³	15.0

The deduced R/Bs are not considered to be satisfactory because the large variability characteristic of the GB-9 fission gas measurements is carried over to them. The V/Rs are considered to be quite good (i.e., $\pm 5\%$), as demonstrated by comparison of laboratory simulation tests of gaseous diffusion transport in the GB-9 fuel rod compared to SLIDER predictions. However, because of breathing due to temperature changes, there are uncertainties in the stability of the gas medium in the GB-9 capsule fuel rod. These difficulties provided the incentive for the improvements introduced into capsule GB-10.

2.1.2. GB-10 Results. The greatly increased capabilities in the sweep gas system of capsule GB-10 permitted, for the first time, the direct measurement of fission gas release from an operating FBR fuel rod. By sweeping gas directly through the fuel region when measuring the R/Bs, and conducting it to the sampling or measuring points, good fission gas release data were acquired at three power levels and cladding outer surface temperatures, namely 39 kW/m (565°C), 44 kW/m (620°C), and 49 kW/m (685°C). Measurements were carried out at burnup intervals of 2.9, 5.1, and 3.2 at. %, respectively, for the power levels indicated. Early measurements were made as described above for V/B measurements in capsule GB-9. Later, the measurements were performed using an on-line Ge(Li) gamma spectrometer mounted in the effluent sweep gas line. Typical R/B and V/B data are shown in Fig. 2 as a function of burnup for Xe-133 and Xe-135m, the longest and shortest half-lived fission products of interest.

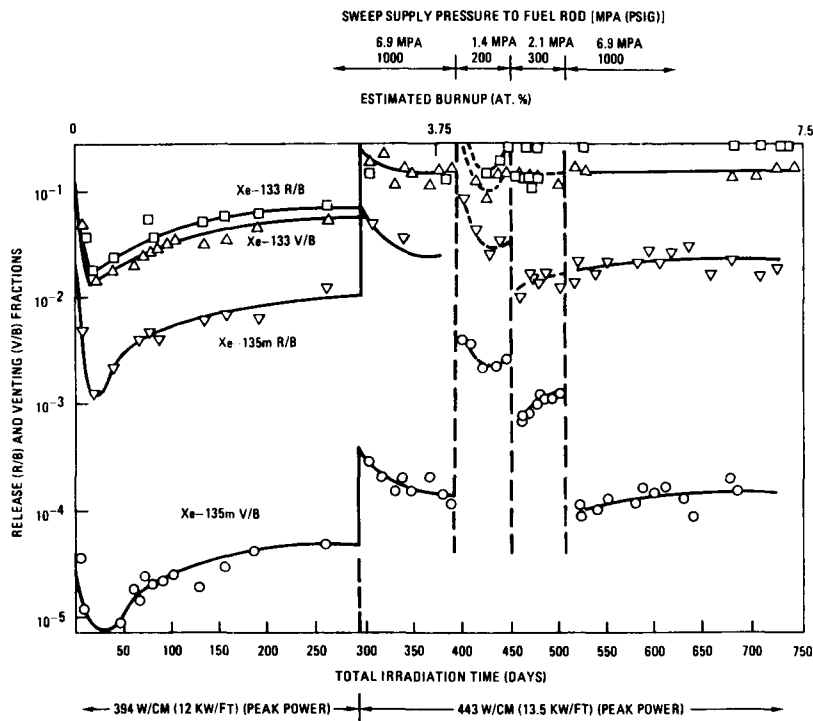


Fig. 2. GCFR capsule GB-10 release (R/B) and venting (V/B) fractions

The effects of changes in power levels, temperatures, and capsule gas pressure are apparent in Fig. 2. When the power level is changed from 39 to 44 kW/m, the transient overshooting of the R/Bs occurred as a consequence of release of fission gas stored in the fuel matrix at the lower power level. The R/B for Xe-133 exceeds a value of 1.0 for a short time. The transient is also observed to last for 2 at. % burnup or longer (see Table V).

The effect of the helium gas pressure in the fuel rod is also apparent in Fig. 2 as the pressure is reduced from 6.8 MPa (1000 psi) to 1.36 MPa (200 psi) to 2.0 MPa (300 psi) and then was returned to 6.8 MPa. The effects of the gas pressure on the V/B and V/R that depend on gas-phase diffusion were anticipated. However, an effect of the gas pressure is also apparent on R/Bs that are dependent upon the solid-state diffusion or migration processes. Again, the effect is transient. Although not of adequate quality to extract quantitative results, the data indicate an area where future research may be fruitful.

TABLE V. IRRADIATION CONDITIONS FOR F-1 (X094) FAST FLUX IRRADIATION EXPERIMENT FUEL RODS

Fuel Rod Identification No.	Pellet Type ^(a)	Fuel O/M	Cladding I.D. Temp (°C)	Linear Rating (W/cm)	Burnup (at. %)	Calculated Exposure, [n/cm ² x 10 ²² (E > 0.1 Mev)]	Surface of Cladding ^(b)	Type of Fission Product Trap ^(c)
G-1	A	1.992	740	453	5.6	3.4	SM	SD
G-2	A	1.971	730	459	5.3	3.4	SM	SD
G-3	A	1.987	669	430	2.7	1.7	SM	SD
G-4	A	1.983	683	456	13.6	6.7	SM	AC
G-5	A	1.990	716	462	5.1	3.4	SM	SD
G-6	A	1.972	662	452	4.9	3.4	SM	AC
G-7	A	1.984	648	472	4.8	3.4	SM	AC
G-8	A	1.985	696	492	10.3	5.6	SM	SD
G-9	A	1.947	706	475	8.9	4.2	SM	AC
G-10	A	1.968	722	495	9.8	4.2	SR	AC
G-11	A	1.968	731	521	9.6	4.2	SR	AC
G-12	S	1.976	714	472	9.7	4.2	SM	AC
G-13	S	1.973	759	521	9.5	4.2	SM	AC

(a) A = annular; S = solid.

(b) SM = smooth; SR = ribbed.

(c) SD = sealed; AC = active.

3. F-1 (X094) FAST FLUX IRRADIATION EXPERIMENT

The first GCFR fast flux irradiation experiment [F-1 (X094)]^(7,8) consisted of seven fuel rods clad in 20% cold-worked 316 stainless steel. The rods were individually encapsulated, with sodium filling the radial gaps between the rod, thermal barrier, and capsule walls. The rods were fueled with (15% Pu, 85% U)O₂ and had depleted UO₂ lower and upper axial blankets and charcoal to trap volatile fission products. The cladding i.d. temperature range covered by these rods was 648° to 759°C (1055° to 1400°F).

The primary objectives of this experiment were to (1) determine fuel irradiation behavior at higher cladding temperature [compared with GCFR design hot-spot midwall temperature of 700°C (1300°F)] to establish the margin in GCFR fuel rod design; (2) compare the behavior of fuel irradiated in a fast flux with fuel irradiated in a thermal flux; and (3) investigate the behavior of charcoal irradiated in a fast flux. The maximum burnup on the lead rod is 13.6% and was reached on March 16, 1976. The test conditions for the experiment are given in Table V.

3.1. Burnups and Behavior of Sol-Gel Fuel in F-1 Fuel Rods

Although additional burnup analyses are under way, experimental results to date are limited to rods G-1, G-2, G-4, G-6, and G-9. The measured burnups based on Nd-148 analyses are compared with calculated values in Table VI.

The fuel used in the F-1 fuel rods was pressed and sintered powder derived from calcined sol-gel char. No particular difference in behavior of the F-1 fuel compared to mechanically blended fuel employed in LMFBR irradiations has been noted to date. Restructuring of the fuel indicates that temperatures and fuel conductivities in the two types of fuel are similar.

3.2. Fission Gas Release From F-1 Fuel Rods

The results of the F-1 fuel rod fission gas extraction and analysis by ANL-E are given in Table VII and are plotted in Fig. 3 as percent fission gas release as a function of rod burnup in atom percent. Fission gas release values for the fuel rods containing active charcoal traps are in the range 64% to 87%; G-8 containing sealed traps had a release value of 66%.

Gas was extracted from fuel pins G-4 and G-13 by drilling into the plenum region and quantitatively transferring the gas to an evacuated pressure-volume measuring and sampling apparatus. Samples of these gases were isotopically analyzed using a mass spectrometer. The amount of

TABLE VI. FUEL BURNUP ANALYSIS

Fuel Rod Identification No.	Location Above Core Bottom [mm. (in.)]	Measured Burnup (at. %)	Calculated Burnup (at. %)
G-1	161.9 (6.375)	5.35	5.18
G-1	317.8 (12.75)	4.35	4.24
G-2	50.8 (2.0)	4.91	4.44
G-2	161.9 (6.375)	5.19	5.05
G-2	317.8 (12.75)	4.26	4.14
G-6	50.8 (2.0)	4.44	4.22
G-6	161.9 (6.375)	4.68	4.78
G-6	317.8 (12.75)	3.95	3.93
G-4	46 (1.81)	12.61	--
G-4	165 (6.48)	13.58	13.1
G-4	322 (12.67)	11.34	--
G-8	159 (6.25)	10.10	12.6
G-9	34.9 (1.375)	8.26	--
G-9	159 (6.25)	8.85	9.7
G-9	321 (12.625)	7.48	--
G-10	159 (6.25)	9.77	10.0
G-11	159 (6.25)	9.63	10.5
G-12	159 (6.25)	9.70	9.6
G-13	84 (3.3)	8.89	--
G-13	159 (6.25)	9.50	10.4
G-13	287 (11.3)	7.94	--

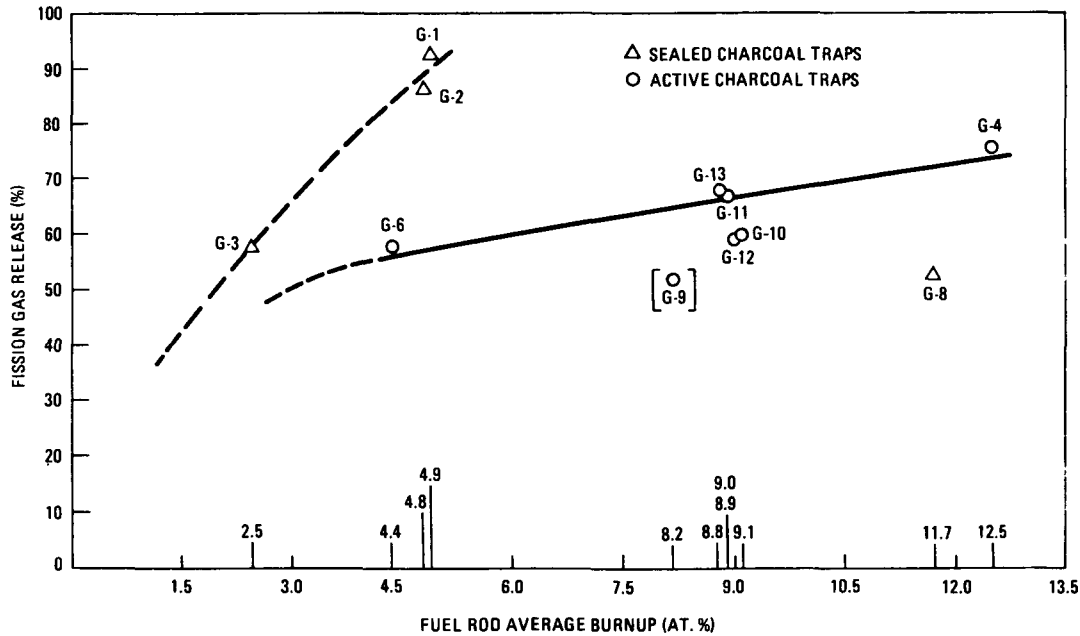


Fig. 3. Fission gas release versus fuel rod burnup

TABLE VII. RESULTS OF GAS SAMPLING AND ANALYSES FOR
F-1 FUEL RODS

	Volume of Gas Extracted (cc at STP)									
	G-1	G-2	G-6	G-4	G-8	G-9	G-10	G-11	G-12	G-13
Fission gas volume, cc	117	112	65	264	176	13	160	174	157	175
Fission gas released to plenum ^(a) , %	104.8	100.4	66.4	87	66	64	75	80	76	79
Peak burnup, at. %	5.6	5.3	4.9	13.6	10.1	8.9	9.8	9.6	9.7	9.5
Fuel O/M	1.992	1.971	1.972	1.983	1.985	1.968	1.968	1.947	1.976	1.973
Clad i.d. max temp, °C	740	730	662	683	696	706	722	731	714	759
Calculated fuel max temp ^(b) , °C	2487	2485	2260	1926	1926	2090	2150	2150	2150	2284

(a) Percent release data are based on measured burnup and fission product inventory values.

(b) The centerline fuel temperatures are calculated based on the run-by-run power data using ANL HECTIC III code for the PIE ANL document issued January 1976. The definition and accuracy of those calculations are unknown at this time. These values relate to the region above reactor midplane. Note the difference in values of rods listed in Table IX.

fission gas collected was compared with the amount of xenon and krypton generated in fission.

It was expected that the recovery value for rod G-9 would be low since activity release to the hot cell stack was noted during the cutting of the rod. Thus, the value for G-9 release (66%) should not be regarded as a quantitatively measured result.

The data presented in Fig. 3 indicate a nonquantitative release (or recovery) of the fission gas. However, a rather well-defined correlation of release and burnup is apparent; this observation has been reported by other workers⁹⁻¹¹. The factors which influence the release of fission gas during irradiation are being characterized and assessed for the F-1 fuel rods.

It is not clear what effect the active fission product trap charcoal has had on these fission gas measurements. It is conceivable that significant amounts of fission gas could be sorbed on the charcoal at STP, i.e., after removal from the reactor. Out-of-pile experiments at GA involving the determination of adsorption isotherms for xenon and krypton indicate that significant amounts of fission gas are adsorbed on the charcoal over the range of ambient to trap operating temperatures and pressures¹². However, since the irradiated charcoal undergoes a 50% to 60% volume shrinkage and has perhaps accumulated a fission product loading greater than 1 wt %, the sorptivity of the charcoal for the fission gases may have been substantially lessened.

The following conclusions are reached from these results:

1. The fission gas release values for the fuel rods containing active traps are in the range 64% to 87%.
2. The release data need to be correlated with metallographic examination to assess the degree of swelling associated with the rods exhibiting lower release values, i.e., G-8.

3.3. Fuel Clad Chemical Interaction in F-1 Fuel Rods

General observations on the fuel clad chemical interaction in the F-1 fuel rods are fairly typical of other high-temperature irradiations. The observed cladding attack in the fuel rods is closer to the recommended fuel cladding chemical interaction (FCCI) correlations for maximum cladding attack rather than nominal attack from the FCCI National Working Group. Fuel rod G-4 (burnup 13.2 at. %) had the maximum depth of cladding attack of ~ 100 μm . Fuel rod G-9 with an O/M ratio of 1.947 had minimal attack.

A typical cladding inner surface is fairly smooth, with some localized region of rather deep interaction. Such localized regions cover a good fraction of the cladding circumference. A reaction product layer in the fuel cladding gap is observed. In some localized regions this reaction product layer has metallic texture. The reaction product layer was not always associated with clad attack.

In addition to the above observations, some anomalous behavior has also been observed. Rod G-8 with 10 at. % burnup showed negligible fuel cladding chemical interaction, whereas a similar rod, G-4 (13.6 at. % burnup), has the maximum clad attack. These observations are being investigated at present.

3.4. Dosimetry and Tritium Analyses for F-1 (X094) Experiment

The dosimeters for the F-1 experiment have been removed from the fuel rods at ANL-MSD and are currently being analyzed. A series of coated fuel particles containing U-238, U-235, and Th-232 isotopes in the dosimeters of the F-1 fuel rod capsules were examined for tritium content. Analysis of these fuel particles for fuel and fission product characterization thus far has confirmed the fast ternary yield for U-235¹³ and has also indicated that tritium yields for U-238, Pu-239, Th-232, and U-233 in a fast flux may be somewhat higher than predicted.

4. F-3 (X206) FAST FLUX EXPERIMENT

The F-3 experiment, which consisted of ten encapsulated GCFR fuel rods with surface-roughened (ribbed) cladding, shared a 19-capsule subassembly with 9 rods from the O8 experiment of Argonne National Laboratory. Temperatures were controlled over the range 675° to 750°C (1250° to 1380°F). Results of a planned interim examination at an exposure of 4.9 at. % burnup and a fluence of 5.2×10^{22} n/cm² show that cladding failures occurred in nine of the ten rods. Investigations showed that the failures were due to defects in the sodium bond between the fuel rod and the capsule.

5. DIAMETRICAL CHANGES IN GCFR FUEL RODS

There are two primary reasons why the diametral changes in GCFR fuel rods can be expected to differ from those in the LMFBR: (1) the GCFR fuel rods are vented and pressure-equalized so that the cladding strain due to fission gas pressure buildup is not present, and (2) the GCFR fuel rods have ribbed cladding. Out-of-pile creep rupture and tensile tests indicate that ribbed cladding tubes are stronger than smooth cladding tubes when compared on the basis of root wall thickness.

5.1. Diametral Changes in GCFR Vented Fuel Rods Irradiated in Thermal Flux

Dimensional measurements on the fuel rods from the vented sweep gas experiment GB-9, which was irradiated to an exposure of 5.84 at. % burnup, showed less than 0.025 mm (0.001 in.) or <0.3% diametral increase. Dimensional measurements on the fuel rod from the vented sweep gas experiment GB-10, which was irradiated to an exposure of 12.11 at. % burnup, showed a diametral increase less than 0.02 mm (0.0009 in.) or <0.2%.

5.2. Diametral Changes in Simulated Vented Rods in Fast Flux

Diameter measurements have been completed on all 13 fuel rods irradiated in the GCFR F-1 (X094) fast flux experiment in EBR-II. The F-1 rods had large plenum to fuel volume ratios (1.4) to simulate venting by minimizing stresses induced by fission gas pressure buildup. The results are summarized in Table VIII. The largest diametral strain of 0.07 mm or 0.9% occurred in rod G-8 in the fueled region at $X/L = 0.63$ above the core bottom (where X/L is the fractional distance above the core bottom). This is one of the three peaks in diametral strain as observed in the 45-deg profilometry trace in a region of ovality (see Fig. 4). The average diametral increase for G-8, ignoring ovality, is 0.05 to 0.06 mm or 0.7% to 0.8% $\Delta D/D$.

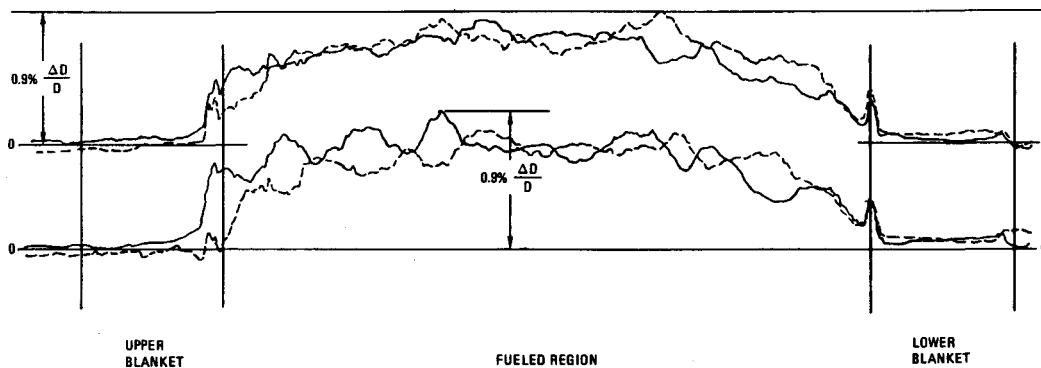


Fig. 4. Profilometry of diameter for rod G-8 at 0°, 90° and 45°, 135° orientations

TABLE VIII. SUMMARY OF PROFILOMETRY RESULTS FOR F-1 RODS IN FINAL PORTION OF X094 IRRADIATION

Fuel Rod Identification No. (Cladding Surface)	Cladding I.D. Temp (°C)	Measured Burnup (at. %)	Calculated Total Fluence [$n/cm^2 \times 10^{22}$ (E = 0.1 MeV)]	Fuel O/M	Smear Density (% of Theoretical Density)	Linear Rating (W/cm)	Original Diam (mm)	Changes in Diam	Diam Increase (%)
G-1 (smooth)	740	5.6	3.4	1.992	82.6	453	7.62	0.02	0.27 ^(a)
G-2 (smooth)	730	5.3	3.4	1.971	84.1	459	7.62	0.02	0.23
G-3 (smooth)	669	2.7	1.7	1.987	85.5	430	7.62	0.02	0.30
G-4 (smooth)	683	13.6	8.0 (6.7)	1.983	82.5	456	7.62	0.05	0.7
G-5 (smooth)	716	5.1	3.4	1.990	83.5	462	7.62	0.02	0.28
G-6 (smooth)	662	4.9	3.4	1.972	82.7	452	7.62	0.02	0.27
G-7 (smooth)	648	4.8	3.4	1.984	82.5	472	7.62	0.01	0.18 ^(a)
G-8 (smooth)	696	10.3	6.8 (5.6)	1.985	86.1	492	7.62	0.07	0.9
G-9 (smooth)	706	8.9	5.1 (4.2)	1.947	84.6	475	7.62	0.03	0.4
G-10 (ribbed)	722	9.8	5.1 (4.2)	1.968	84.2	495	7.82	0.03	0.4
G-11 (ribbed)	731	9.6	5.1 (4.2)	1.968	84.3	521	7.82	0.04	0.5
G-12 (smooth)	714	9.7	5.1 (4.2)	1.976	84.3	472	7.62	0.04	0.5
G-13 (smooth)	759	9.5	5.1 (4.2)	1.973	84.4	521	7.62	0.05	0.6

^(a) Maximum diametral changes occurred at cesium peaks near fuel blanket interface for rods G-1 and G-7.

All of the smooth fuel rods (G-1 through G-9, G-12, and G-13) showed peaking in diameter at the fuel/blanket interfaces and several showed a peak at the bottom end of the lower blanket column. The two ribbed rods G-10 and G-11 showed little or no peaking of diametral increase at the fuel/blanket interface and only one trace (90 deg) showed a peak at the top of the upper blanket. It has previously been shown that peaking in diameter increase is associated with localized Cs-137 peaks in the gamma scans of the fuel rods. Localized peaking in diameter in the fuel region seems to be ovality and is associated with peaks in gross gamma scans.

Rod G-4, with the lowest smear density (82.5% TD) and highest burnup (13.6 at. %), had the largest diametral increase peaks at the blanket end and at the axial fuel/blanket interface (see Fig. 5). Rod G-8, with the highest smear density (86.1% TD) and burnup of ~ 10 at. %, showed a greater step increase in diameter at the fuel/blanket interface and had the largest diameter increase of any of the F-1 rods. Rod G-9, with low O/M (1.947), had the smallest diameter increase of the smooth rods (see Fig. 6), less ovality in the fuel region, and significant peaking in diametral increase and ovality in the upper blanket region. The profilometries of the two ribbed rods G-10 and G-11 (see Figs. 7 and 8) were similar in appearance except that in G-11 there was a dip in the profilometry traces at $X/L = 0.15$ and a peak at the top of the upper blanket in only one trace (eight azimuthal traces were made; the second four at 180° , 225° , 270° , and 315° are a check on the first four made at 0° , 45° , 90° , and 135°). The profilometry traces in the fueled region of these ribbed rods were unusually flat compared to the smooth rods, even though the diameter increases were equal to those found in the smooth rods G-9 and G-12. Compared to the other F-1 rods, rod G-12 (see Fig. 9) had intermediate diameter increase with peaks at the fuel blanket interface and medium ovality. Rod G-13 (see Fig. 10), the highest temperature rod (cladding temperature of 759°C), had the largest diameter increase of the five replacement fuel rods (G-9 through G-13). (Rods G-1 through G-8 were fabricated for the initial loading, and rods G-9 through G-13 were fabricated as replacements for rods removed during interim examinations.) A significant diameter increase peak is seen at the lower fuel/blanket interface of rod G-13, ovality occurred above the core midplane, and larger ovality occurred in the upper blanket region.

Fuel rods G-9 through G-13 (with 7.7 at. % burnup exposure) show a $\Delta D/D$ which seems temperature-dependent (the strain increases with increase in operating temperature; see Fig. 11). The uniform diametral increases (along the fueled length) of ribbed rods G-10 and G-11 is likely due to the strengthening effect of the ribs.

5.3. Diametral Changes in Ribbed Rods Compared to Smooth Rods

The profilometry data from F-1 fuel rods have been presented in Table IX in the form of average outside diameter for four equal fueled

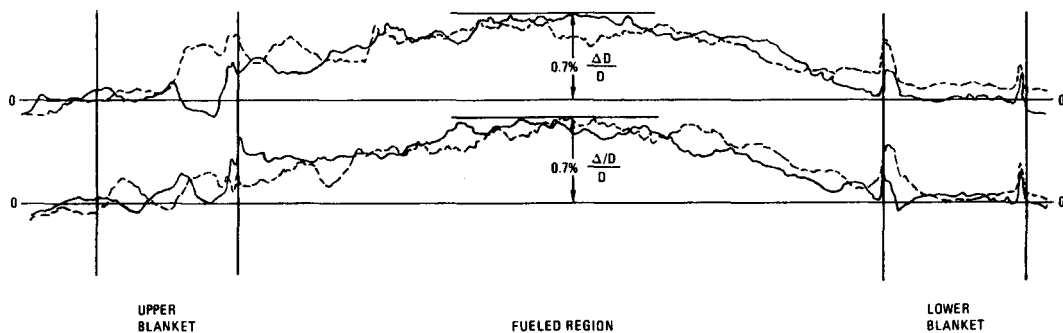


Fig. 5. Profilometry of diameter for rod G-4 at 0°, 90°, and 45°, 135° orientations

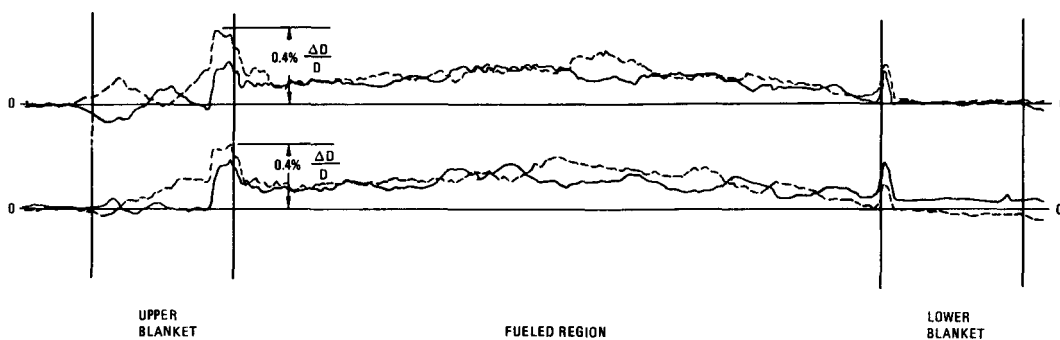


Fig. 6. Profilometry of diameter for rod G-9 at 0°, 90° and 45°, 135° orientations

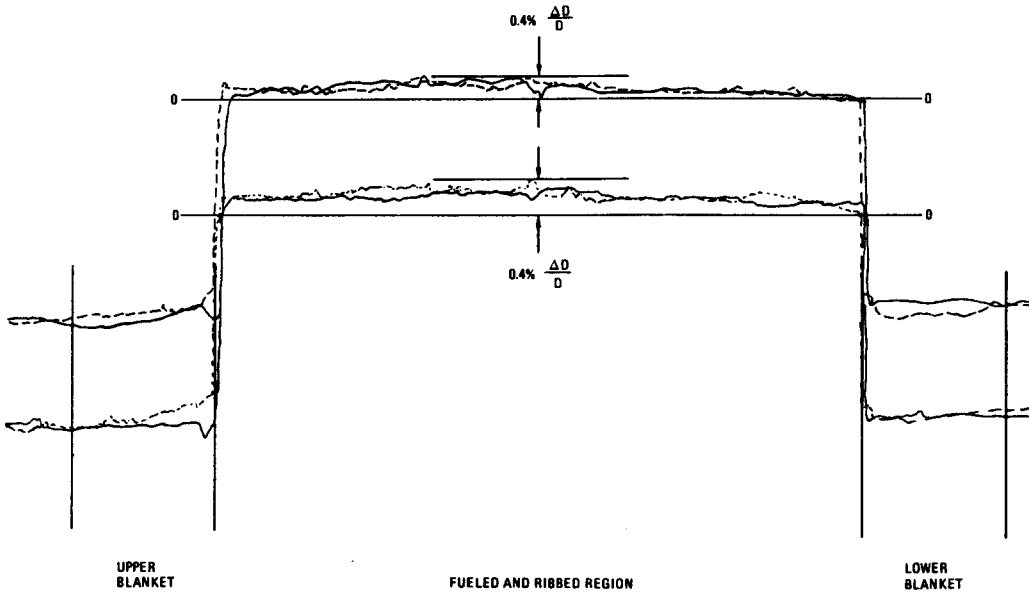


Fig. 7. Profilometry of diameter for rod G-10 (ribbed cladding) at 0°, 90° and 45°, 135° orientations

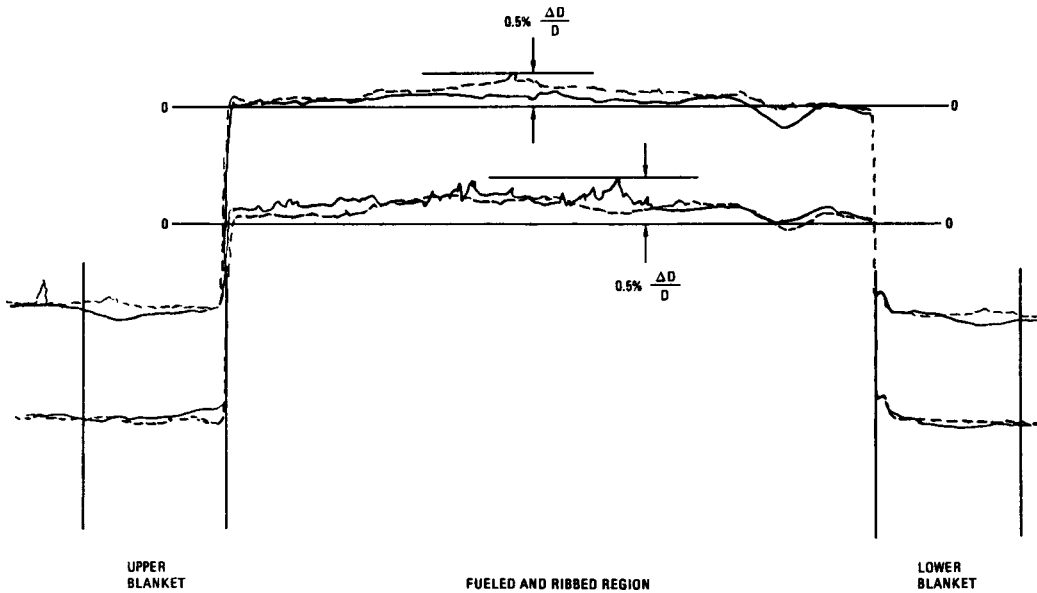


Fig. 8. Profilometry of diameter for rod G-11 (ribbed cladding) at 0°, 90° and 45°, 135° orientations

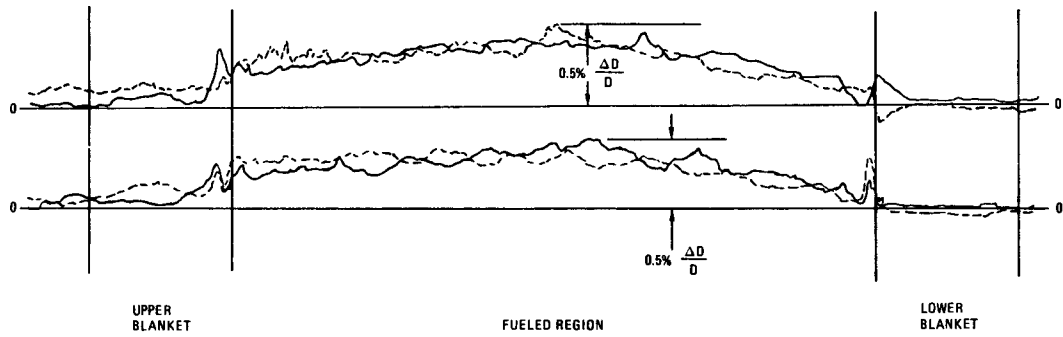


Fig. 9. Profilometry of diameter for rod G-12 at 0°, 90° and 45°, 135° orientations

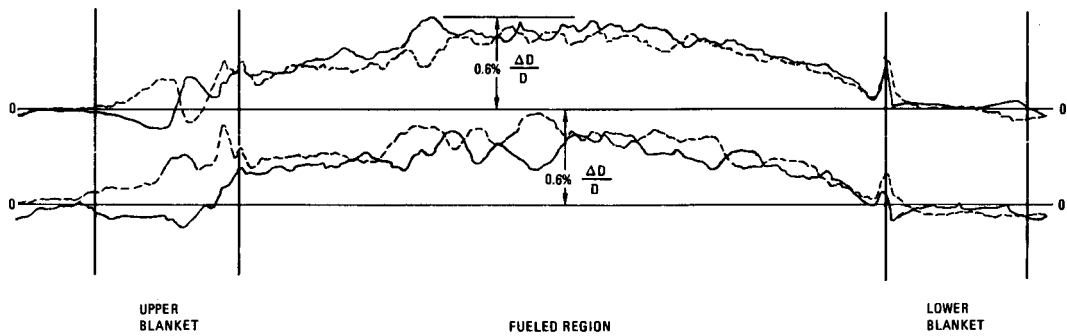


Fig. 10. Profilometry of diameter for rod G-13 at 0°, 90° and 45°, 135° orientations

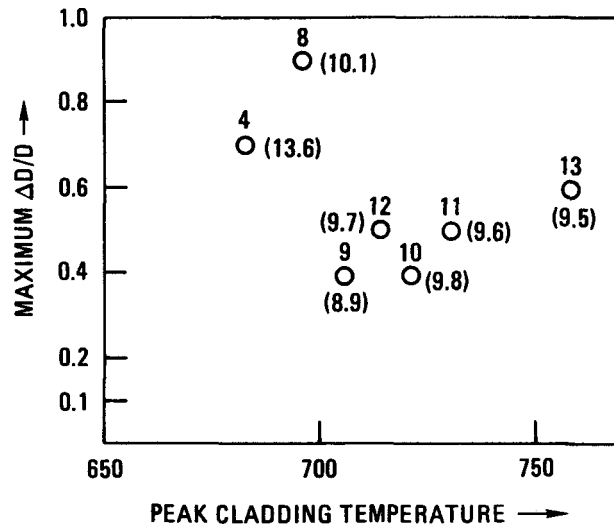
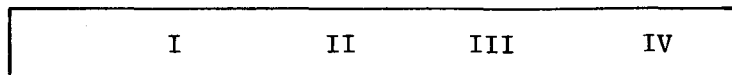


Fig. 11. Plot of diametral increases versus maximum cladding temperature during irradiation for the F-1 (X094) fuel rods. Numbers in parentheses are exposure values in atom percent.

TABLE IX. PROFILOMETRY DATA (CONDENSED) FOR F-1

Rod No.	Average Diameter (mm)				Maximum Diameter (mm)
	I	II	III	IV	
G-1	7.64	7.64	7.64	7.64	7.65
G-2	7.63	7.64	7.64	7.64	7.64
G-3	7.64	7.65	7.65	7.64	7.65
G-4	7.65	7.66	7.66	7.66	7.67
G-5	7.63	7.64	7.63	7.64	7.65
G-6	7.63	7.64	7.63	7.64	7.64
G-7	7.63	7.64	7.64	7.64	7.64
G-8	7.66	7.67	7.68	7.67	7.69
G-9	7.64	7.64	7.65	7.64	7.65
G-10	7.84	7.84	7.85	7.84	7.86
G-11	7.84	7.85	7.86	7.85	7.86
G-12	7.65	7.65	7.65	7.65	7.66
G-13	7.65	7.66	7.66	7.65	7.67



BOTTOM FUEL ROD TOP

342.9 cm (13.5 in.)

sections of the rods. All rods except G-10 and G-11 had a nominal o.d. of 7.62 mm (0.300 in.) prior to the irradiation. Rods G-10 and G-11 were ribbed, with a nominal preirradiation o.d. of 1.82 mm (0.308 in.). All 7.62-mm (0.300-in.) o.d. rods were fabricated from cladding belonging to heat V87210, which is the same heat as the N-lot material. The N-lot material has an incubation period of 8×10^{22} nvt for swelling. The other cladding [7.82 mm (0.308-in. o.d.)] also belongs to the original developmental cladding lots. Thus, no swelling can be expected in the F-1 cladding, and the profilometry data give the value for the sum of the thermal and irradiation creep strains. From these limited data, no significant difference in diametral strain of ribbed compared to smooth rods is apparent. Except as noted in Section 5.2 above, the diametral strain is more uniform in the ribbed rods.

5.4. Diametral Changes in GCFR Rods Compared to LMFBR Rods

The F-1 fuel rod diametral changes were compared to LMFBR rods with similar irradiation conditions (HEDL P-23 B and P-23 C¹⁴). The maximum diametral changes due to irradiation were considerably less in the F-1 rods than in the P-23 rods because the plenum to fuel volume ratios were larger in the F-1 rods (1.3 to 1.4) compared to the P-23 rods (1.09). This phenomenon is readily explainable from LIFE III analyses. Since the F-1 and P-23 fuel rods were subject to similar irradiation conditions, it is concluded that the fuel cladding mechanical interaction effect on the diametral changes is the same, provided the fuel rods were fabricated similarly. Therefore, the higher plenum gas pressure in the smaller plenum of the P-23 fuel rods gave rise to higher cladding diametral changes.

6. F-5 (X317) GRID-SPACED FUEL ROD BUNDLE EXPERIMENT IN EBR-II

6-1. F-5 Description

The GCFR F-5 (X317) grid-spaced fuel rod bundle experiment consists of 31 fuel rods and 6 coolant bypass tubes for the initial loading. The principal objectives of the experiment are to investigate (1) fuel rod performance under simulated GCFR conditions of power rating, cladding temperatures, fuel rod diameter, ribbed cladding, and fuel temperatures, (2) fuel rod performance during power changes that simulate the 180-deg rotation of an assembly at the GCFR core/blanket interface, and (3) the performance of a prototype grid-spaced bundle structure. The 20% cold-worked 316 stainless-steel-clad, (Pu-U)₂O₇ fueled rods have ribbed surfaces. The linear heat generation rating for the rods is 400 W/cm, and the peak cladding midwall temperature is approximately 700°C. The GCFR F-5 (X317) experiment is now being irradiated in row 5 of EBR-II.

The overall F-5 (X317) fuel rod is shown in Fig. 12. The F-5 (X317) grid spaced bundle design is shown in Fig. 13. The design data for the fuel rods are listed in Table X, and the variables being tested are listed in Table XI. The irradiation plan, showing the distribution of the different types of fuel rods and the planned exposures, is given in Fig. 14.

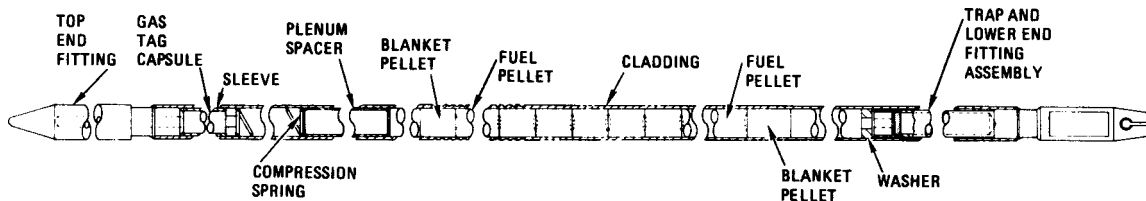


Fig. 12. GCFR F-5 fuel pin assembly

The special components for the fuel rods, the dosimeters*, and the grid-spaced bundle required for the initial loading of the experiment were fabricated at GA. The fuel was made and the rods were assembled at HEDL.

6.2. F-5 Status/Plans

Final assembly of the F-5 (X317) experiment employing the hardware fabricated and assembled by GA and the (Pu-U) O_2 fueled rods assembled by HEDL was completed at the EBR-II site on January 5, 1978; the final assembly is shown in Figs. 15 and 16. Irradiation of the experiment was started in EBR-II run 93 (row 5 position) on January 21, 1978. The final goal burnup is approximately 10 at. %,** and the experiment is expected to have achieved an exposure of approximately 4 at. % at the time of the Monterey conference toward an exposure goal of 5.0 at. % in the first full-power phase of its irradiation. Upon reaching the exposure of 5 at. %, the experiment will undergo an interim examination and will be constituted into a 19-rod bundle for the low-power (240 W/cm²) phase of its irradiation. The grid-spaced skeleton required for the reconstitution is being fabricated and assembled. Following reconstitution and low-power exposure of approximately 1 at. %, another interim examination will be performed. The experiment will then be reconstituted into a 31-rod

*Dosimeters containing metal wires and coated particles with spheres of Pu-239, U-235, U-233, U-238, and Th-232 containing oxides and carbides (double-encapsulated) are used to measure fluence distribution and tritium yield. The Pu-239-containing particles were encapsulated at ORNL.

**This goal may be extended to cladding breach provided the EBR-II operating schedule permits the extension.

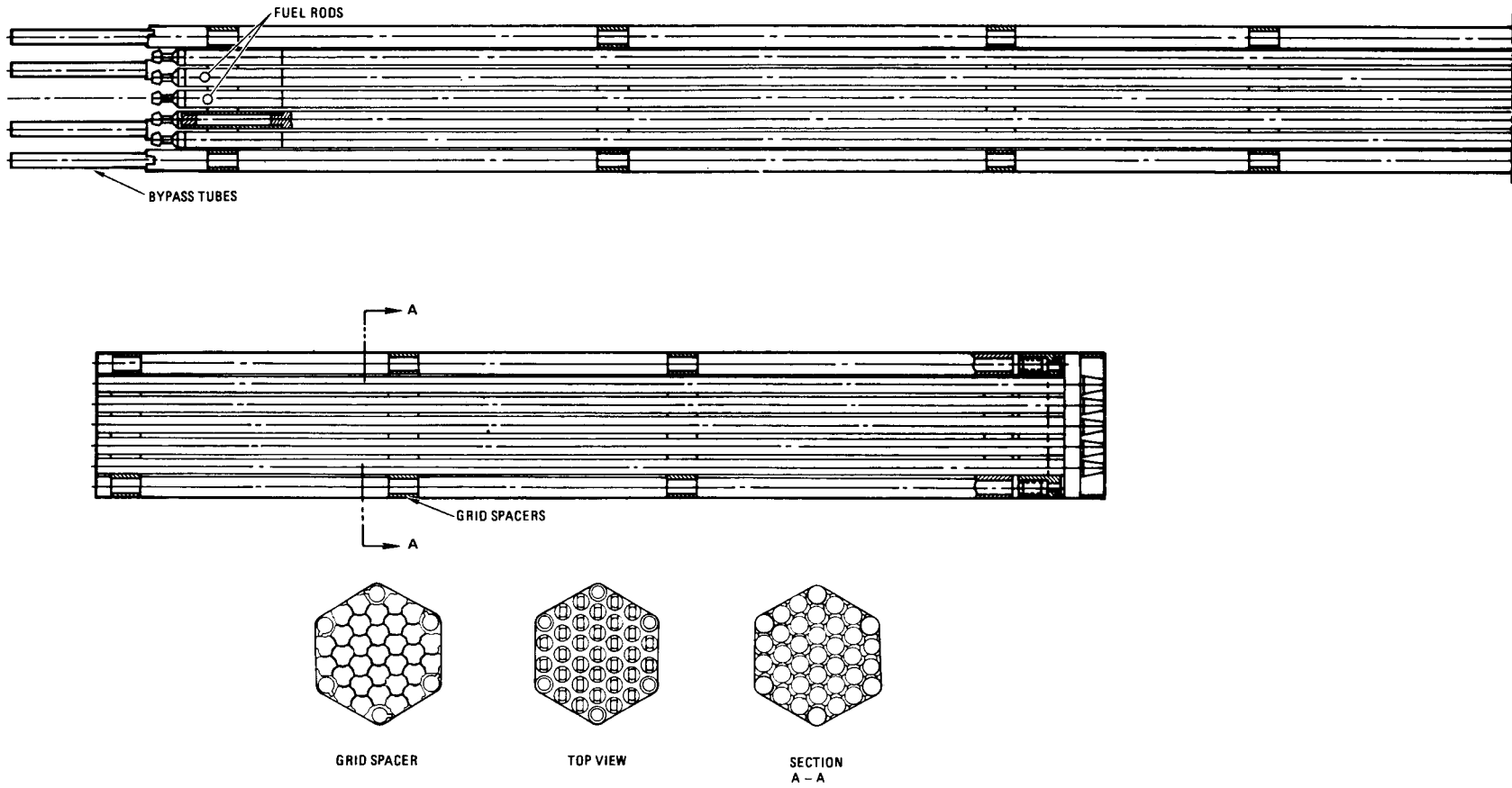


Fig. 13. The F-5 (X317) grid-spaced bundle design

TABLE X. FUEL ROD DESIGN DATA

<u>Cladding</u>	
Material	316 SS, 20% cold worked
Diameter, o.d. x i.d.	7.46 x 6.44 mm (0.2937 x 0.2535 in.)
Rib o.d. x width	7.46 x 0.45 mm (0.2937 x 0.0177 in.)
Rib spacing (pitch)	1.56 mm (0.0614 in.)
Length of ribbed section	270 mm (10.63 in.)
Element length	1041 mm (41 in.)
Plenum volume	10.6 ml
<u>Fuel</u>	
Pellet o.d. x length	6.30 x 8.0 mm (0.2480 x 0.3150 in.)
Sintered density	89.3% ± 2% TD
Smear density	88% ± 5% TD
Composition:	
UO ₂ /(UO ₂ + PuO ₂)	75%
Enrichments:	
U-235/U	36%
(Pu-239 + Pu-241)/Pu	88.3%
O/M ratio	1.96
Fuel length	343 mm (13.5 in.)
Fuel weight	104 g
<u>Blanket (axial)</u>	
Pellet o.d. x length	
Standard	6.30 x 11.4 mm (0.2480 x 0.450 in.)
Modified	6.30 x 6.8 mm (0.2480 x 0.2677 in.)
Material	Depleted UO ₂
Sintered density	
Standard	93% ± 2% TD
Modified	80% ± 2% TD
Blanket length	
Top	120 mm (4.7 in.)
Bottom	48 mm (1.9 in.)

TABLE XI. FUEL ROD NOMENCLATURE DENOTING DESIGN VARIABLES

Fuel Rod Prefix Designation	Trap Material		Blanket (a)		TED (b)	
	Charcoal	Graphite	Standard	Modified	Yes	No
GA 30 through 49	X		X			X
GB ^(c) 50 through 51	X		X		X	
GC 52 through 59		X	X			X
GD 60 through 63		X	X		X	
GE 64 through 70	X			X		X
GF ^(c) 71 through 72	X			X	X	
GG 73 through 75		X		X		X
GH 76 through 77		X		X	X	

- (a) Standard: All blanket pellets are ~93% TD.
 Modified: The four pellets nearest the fuel (two at top and two at bottom) are ~80% TD; remaining pellets are ~93% TD.
- (b) TED = thermal expansion device for temperature monitoring.
- (c) Not contained in initial loading.

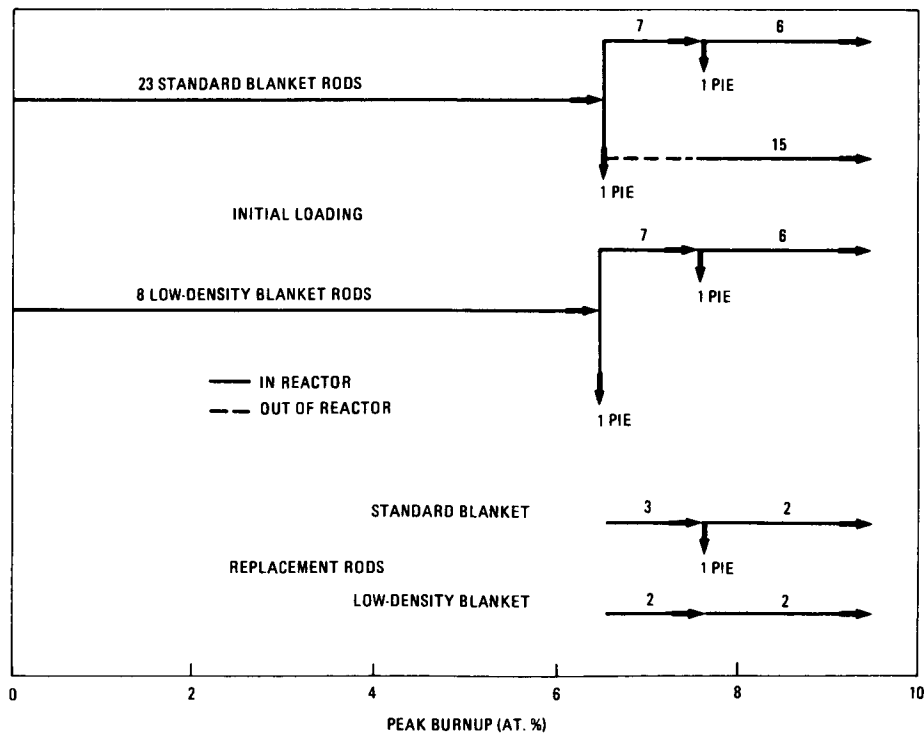


Figure 14. Summary of F-5 irradiation plan showing fuel rods

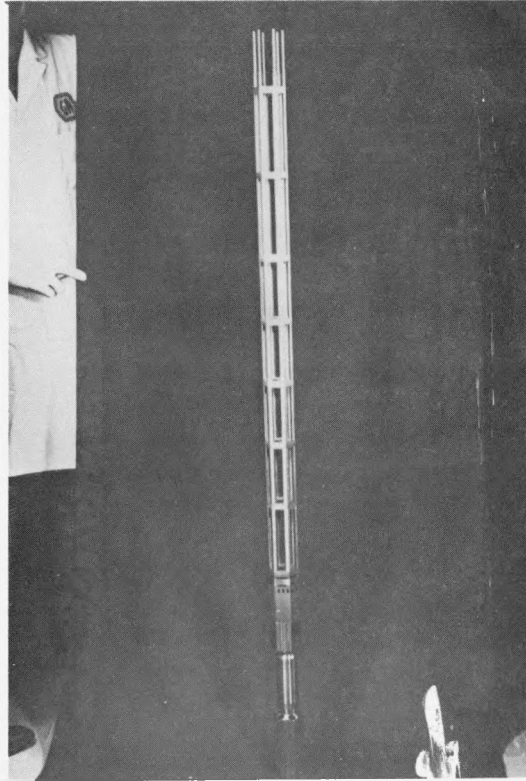


Fig. 15. F-5 grid-spaced bundle skeleton after assembly

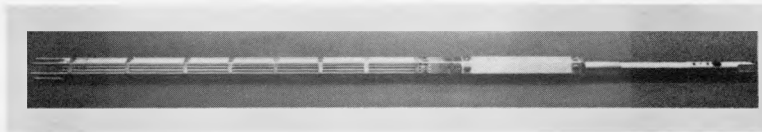


Fig. 16. F-5 (X317) grid-spaced fuel rod bundle after final loading with cold-worked 316 SS clad, $(\text{Pu-U})\text{O}_2$ fueled rods at EBR-II

assembly for full-power operation to the final goal burnup of approximately 10 at. %. The grid spacer hardware components for the 31-rod reconstitution are also being fabricated.

7. HELM SERIES OF VENTED ROD BUNDLE IRRADIATIONS IN BR2 AT MOL

The details of the design, fabrication, and operation of the HELM series of GCFR 12-rod bundle tests are given in Part 2 of this combined paper entitled, "Irradiation of Gas-Cooled Fast Reactor Test Fuel Bundles in the BR2 Helium Loop-Mol," by W. Krug et al.

8. CONCLUSIONS

1. The performance of vented rods irradiated in a thermal flux (ORR) has been excellent and has provided useful data for verification of fission gas release models and for volatile fission product behavior.
2. Irradiation tests of GCFR simulated vented single rods in fast flux (EBR-II) have indicated lower diametral cladding strain than LMFBR fuel rods. The difference is attributed to absence of fission gas pressure-induced stress on the cladding on the GCFR fuel rods.
3. There appears to be no measurable difference in the performance of ribbed compared to smooth rods based on the data obtained from the GCFR irradiation tests to date.
4. Testing of 12-rod vented bundles in the helium loop at Mol is providing operational data on gaseous and volatile fission product release and behavior under steady-state and breathing conditions, the helium purification system performance, hydrogen and moisture control in the helium, and permeation and venting of tritium. Measured and observed results to date verify the expected performance of GCFR vented bundles.

REFERENCES

1. R. H. Simon et al., "Gas-Cooled Fast Reactor Fuel-Element Development," paper presented at International Meeting on Fast Reactor Fuel and Fuel Elements, Karlsruhe, Germany, September 28-30, 1970 (GA-10262, August 7, 1970).
2. U. Gat and P. R. Kasten, "Gas-Cooled Fast Reactor Program Progress Report for Period July 1, 1975 through December 31, 1976," ERDA Report ORNL-5294, Oak Ridge National Laboratory, December 1977.
3. J. R. Lindgren et al., "Fast Flux Irradiation Experiments Performed at High Temperature," Special Issue, "GCFR Engineering and Design," Nuclear Engineering and Design 40, 171-190 (1977).
4. J. R. Lindgren, P. W. Flynn, and L. C. Foster, "Fabrication of Grid-Spaced Bundle for the F-5 (X317) Irradiation Experiment," ERDA Report GA-A15056, General Atomic Company, to be published.
5. R. V. Strain, C. W. Renfro, and L. A. Neimark, "Post Irradiation Examination of the GB-9 Element," Argonne National Laboratory Report ANL-8067, October 1976.
6. K. B. Jadhov and B. W. Roos, "SLIDER, A Fortran V Program for the Computation of the Release of Fission Products from One-Dimensional Multilayered Fuel Configurations," USAEC Report GA-8566, Gulf General Atomic, August 1969.
7. R. V. Strain, "Post Irradiation Examination of Element G-3 from the GCFR F-1 Series of Mixed Oxide Elements after 3 Atom Percent Burnup," Argonne National Laboratory Report ANL-76-128, to be published.
8. R. V. Strain and C. E. Johnson, "Post Irradiation Examination of Fuel Pins from GCFR F-1 Series of Fuel Pins after 5.5 Atom Percent Burnup," Argonne National Laboratory Report ANL-76-129, May 1978.
9. W. H. McCarthy, "Low Power, Moderate Burnup, Fast Irradiation of (U,Pu)O₂ Fuels, Series F6 and F8," General Electric Company Report GEAP-14098, June 1976, pp. 45-47.
10. R. F. Hilbert et al., "Irradiation Performance of Wire-Wrap Spaced-Fuel Rods (Series F9)," General Electric Company Report GEAP-14069, July 1975.
11. G. R. Baird et al., "Fabrication, Irradiation and Postirradiation Examination of Mixed Oxide Fuel Pins," HEDL-TME-76-16, Hanford Engineering Development Laboratory, April 1976, pp. 6-64.

12. "Gas-Cooled Fast Breeder Reactor Quarterly Progress Report for the Period November 1, 1968 through January 31, 1969," USAEC Report GA-9229, Gulf General Atomic Company, March 24, 1969.
13. P. P. Larsen et al., "Chemical Engineering Division Burnup, Cross Section, and Dosimetry Semiannual Report, January-June 1972," Argonne National Laboratory Report ANL-7924, 1972, pp. 18-21.
14. "LMFBR Fuels," HEDL Monthly Newsletter, TC-260-28, April 1977.

PART 2. IRRADIATION OF GCFR TEST FUEL BUNDLES IN THE BR 2 HELIUM LOOP-MOL

H. EURINGER and W. KRUG

Kernforschungsanlage Jülich, Germany

W. JUNG

Kernkraftwerkunion Erlangen, Germany

G. VANMASSENHOVE

Centre d'Etude de l'Energie Nucléaire, Mol, Belgium

R. J. CAMPANA

General Atomic Company, San Diego, California

PART 2. IRRADIATION OF GCFR TEST FUEL BUNDLES
IN THE BR2 HELIUM LOOP-MOL

1. INTRODUCTION

The gas cooled fast breeder reactor will employ many features of the fuel element concept of the sodium cooled fast breeder. For example, the same cladding material will be used for the fuel rods. In Germany the material is 1.4981, and in the USA cold worked 316 SS. For these kinds of steel the effect of fast neutrons, which is independent of the cooling medium, is well known and applicable to a GCFR. Nevertheless, a fuel element bundle has to be tested, cooled in flowing helium to ensure that the heat can be carried away adequately, to learn about vibration of the pins, the interaction between spacers and fuel rods, the chemistry inside the pins near the cladding and so on, and last but not least, to obtain knowledge about the release of fission products via the venting system and the operation and handling of the fission gas cleanup system.

The loop experiments, which are performed within the GCFR program of the the Federal Republic of Germany together with Belgium, are named HELM 1, 2, and so on. The third experiment of this series is under irradiation now. It is the first integral test of the GCFR bundle and may be regarded as the key experiment on the way to the construction of a GCFR demonstration plant. It is the only planned GCFR helium loop experiment. The firms participating in this experiment are:

- KFA, Kernforschungsanlage Jülich, Germany
- KWU, Kernkraftwerkunion Erlangen, Germany
- CEN-SCK, Centre d'Etude de l'Energie Nucléaire, Mol, Belgium,

in cooperation with:

- GA, General Atomic, San Diego, USA
- KFK, Kernforschungsanlage Karlsruhe, Germany

2. COMPARISON WITH A DEMO PLANT

The HELM irradiations are carried out in the reactor BR2 in Mol, Belgium. Table I shows a comparison of the most important parameters of the bundle tests and of the GCFR demonstration plant. The principal differences are the fuel length, which has a minimum influence on the results, and the fast fluence. Other operating conditions and the length of the upper blanket, which does influence the fission gas release, are well simulated in this test.

TABLE I
COMPARISON OF LOOP AND REACTOR PARAMETERS

	He Loop-Mol	Demo Plant
Number of rods per bundle	12	265
Outer rod diameter, mm	8.0	7.4
Rod surface	Artificially roughened	
Fuel length, mm	600	1130
Blanket length, mm	420	450
Rod trap length, mm	50	76
Fuel	(U,Pu)O ₂	(U,Pu)O ₂
Cladding material	1.4981 (316 SS)	316 SS
Max gas temperature, °C	500	580
Operation pressure, MPa	60	86
Max cladding temperature, °C	680	639
Lin. rod power, kW/m	45	33
Max burnup, MWd/kg	100 (60) (a)	100
FE seal bypass	Piston rings	
Seal vent connection	Metal to metal cone	
Flow at vent connection, g/s	0 - 1	0.15
Fast fluence, 10 ²² /cm ²	2.6	24

(a) Design burnup is 100 MWd/kg; initial goal is 60 MWd/kg.

3. CONSTRUCTION OF THE FUEL ELEMENT

3.1. Fuel Element Bundle

Since the fuel element bundle consists of a total of 12 rods, only three of them are inner rods. To simulate inner rod conditions in the other nine, the bundle is surrounded by a flow guide tube with an adjusted profile so that the outer rods have almost the same temperature distribution

as the inner ones. The fuel inside the rods consists of a (U, Pu)O₂ mixture with 15% Pu. Because the irradiation is being done in a side channel of the BR2 with a high flux gradient, two uranium enrichments had to be chosen (90% and 75%) to obtain similar power in each rod. The blanket zones at both ends of the rods contain natural UO₂. The cladding of the rods is roughened in the fuel region by a helical rib to improve the heat transfer to the cooling gas. At the upper end of each rod a charcoal filter to trap aerosols and delay gaseous fission products is located. The rods are screwed into a venting manifold at its top; this connection method proved to be gastight. In the venting manifold, the fuel rods are interconnected by a channel system. From there a small gas tube leads to a larger common charcoal trap and then to the head of the bundle. This head consists of a handling device and a conical expansion with three pads, on which the bundle rests on an inner cone of a support tube.

3.2. In-Pile Section

The in-pile section (IPS) with its double-wall pressure tube surrounds the fuel element bundle. The coolant gas enters the IPS from beneath, reverses flow above the fuel element bundle, and cools it on its way downward. The IPS is surrounded by a Cd screen and a ten-tube driver fuel element. This arrangement results in an epithermal spectrum and a flat power distribution over the rods as in the fast flux of a demonstration plant.

3.3. Pressure Equalization System

The function of the pressure equalization system (PES) (see Fig. 1) is of particular importance to the GCFR. The fuel element bundle, which is inserted into the IPS from above, is supported on a cone of the support tube. This tube, which is fixed beneath, separates the cold and hot cooling gas. The fuel element bundle is partially sealed by two piston rings at the top head to provide a small gas bypass between support tube and guide tube. The fission gas line from the common charcoal trap is connected to one of the three pads at the bundle head, which conform to the configuration of the cone of the support tube. On the downstream side, the fission gas line goes from the cone of the support tube, out of the reactor, to the fission gas cleanup system. Near the pad, over which the active gas passage is connected, a 1-mm hole is drilled from outside into the fission gas line. This is the so-called suction hole. Through this drilled hole a steady stream of helium carries away the fission products, which reach this location by diffusion during steady-state conditions.

The coolant gas pressure drop through the bundle is about 0.1 MPa. The gas pressure inside the fuel rods is about equal to the coolant gas pressure at the exit of the bundle. At this pressure, the interior is connected via the suction hole and the fission gas line through the gap

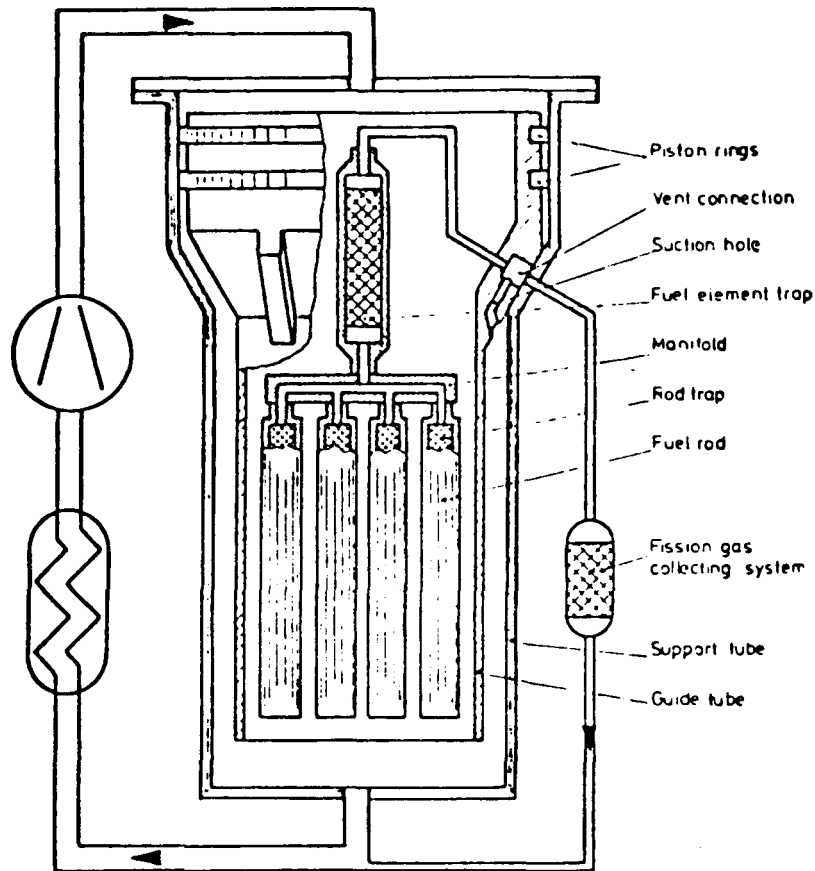


Fig. 1. Principle of pressure equalization system

between the guide tube and support tube. Thus, the coolant gas pressure outside the bundle is somewhat higher than the pressure inside the rods at all locations. Should a small leak arise in the cladding, an inward gas stream would sweep the fission gases out of the reactor into the fission gas cleanup system. By analyzing the fission gas spectrum in this system, a leak can be detected and, by appropriately making interconnections in the PES, a leaking fuel assembly in a reactor can be located.

The pressure equalization system provides the following benefits:

1. The cladding of the fuel pins is not stressed by the high external coolant pressure at the beginning of life or an internal fission gas pressure buildup from production of fission gases as burnup progresses. A failure of the cladding is thus less likely. As a major benefit, a fission gas plenum is not necessary.

2. A large fraction of gaseous fission products leaves the bundle through the fission gas line (especially the longer lived ones). As a result, the fission gas inventory in the reactor is reduced.
3. If a breach occurs in the fuel rod cladding, fission gases are not released to the cooling gas under normal operating conditions.

4. PRELIMINARY EXPERIMENTS

Before discussing the results of the actual irradiation of bundle HELM 3, the experiments preliminary to this test should be discussed. For the thermo-hydraulic design of the 12-rod bundle, full scale tests with an electrically heated dummy bundle were performed in Karlsruhe. Using the results of these tests, the size and shape of the shroud tube were determined with the constraint that the temperature gradient should not be larger than 30°C for any fuel rod. Grid spacers were positioned along the length of the rods to maintain the required configuration and position. By applying the SAGAPO code, the temperature distribution in the bundle, the interdependence of cooling gas outlet temperature, inlet temperature, flow through the bundle, and pressure drop were calculated. The hot spot temperature of the bundle was calculated after a short operating interval, and the conditions were set so the cladding temperature did not exceed 680°C.

The second preliminary test was the operation of the mockup dummy test facility in Jülich. A small loop with a gas bearing blower/circulator and a test bundle with stainless steel pins was constructed to test the bundle under realistic conditions (60 bars, 350°C, 220 g/sec of helium flow). The thermodynamic and mechanical behavior of the test bundle was good, as expected, during a two-month test, so the development of the bundle was completed as scheduled.

The next bundle test was performed in the BR2 reactor facility in Mol with stainless steel pins to test the whole installation, train the personnel, measure the γ -heating and the activation of He3. The activation turned out to be negligible based on tritium measurements in the helium. This bundle HELM 1 was irradiated for 3 cycles of the BR2.

The first fueled bundle HELM 2 (with UO₂ pellets but without Pu) provided all the operating conditions expected from the main Pu fueled bundle. The results allowed us to make final corrections to the experiment design and verify all measuring methods.

Measurements of fission gas release from the bundle to the fission gas cleanup system and the main coolant gas were made. During steady state conditions the following venting over birth ratio (V/B) values were measured (at normal full power conditions):

	Fission gas cleanup system	Main cooling gas
Xe-131	5.10^{-2}	*
Xe-133	2.10^{-2}	7.10^{-6}
Xe-133m	5.10^{-3}	*
Xe-135	5.10^{-5}	4.10^{-8}
Kr-85m	3.10^{-5}	3.10^{-8}
Kr-88	2.10^{-6}	*

The major fraction of the activity released to the fission gas cleanup system is from the isotopes Xe-133, Xe-135, and Kr-85, even though they have low absolute V/B values. From these results it can be concluded that only 2.10^{-5} of the gaseous activity released from the fuel is swept to the vented gas system. The fission gas inventory in the fuel pins is reduced by a factor of two by radioactive species decay, because the main delay takes place in the charcoal traps. The activity in the main loop is low and in the range of that expected for an HTR. The source of this activity is not quite clear at the moment. It is independent of the flow through the vented gas system and it contains a relatively high fraction of short lived isotopes.

When the temperature of the coolant gas and the temperatures of the pins are increased, or the pressure of the gas is decreased, the bundle exhales fission gases. This exhalation of fission gas takes place in two steps, with the activity passing through two maxima. In the first activity maximum, the shorter lived isotopes of Kr are found. The second maximum includes the longer lived Xe isotopes. With the excursions of temperature and pressure expected for a GCFR demonstration plant, the activity will never exceed five times the activity during normal operation based on these results.

* Not measurable.

To determine how much the flow through the suction hole can be reduced, we lowered the flow to 0.05 g/sec without an increase in the V/B value of the coolant gas. Thus, the energy consumption for liquid nitrogen (LN) cooling in the fission gas cleanup system can be reduced to a very low value when the small V/B values are taken into account.

5. RESULTS

The first results from the HELM experiments, which seem to be important, are reported in the following sections.

5.1. Tritium

Extensive tritium measurements were carried out to obtain knowledge of the extent and location of tritium produced by fission. If this tritium does not remain inside the fuel pins, it must be removed from the GCFR primary coolant. For this reason, a method for measuring tritium in the fission gas cleanup system as well as in the cooling gas was provided. It is also necessary to know the chemical form, whether it is HT or HTO. The results obtained to date show that tritium produced by activation of He3 is negligible, but more than 85% of the fission product tritium is released to the He gas. The fractions of tritium in the fission gas cleanup system and in the cooling loop are 25% and 75%, respectively. The chemical form depends on the H₂ and H₂O levels in the cooling gas (H₂ and H₂O are added by an injection system. The current level is 30 vpm for H₂O and 90 vpm for H₂.)

	H ₂ and H ₂ O lower than 5 vpm (%)	H ₂ O and H ₂ higher than 15 and 50 vpm, respectively (%)
HTO to the main cooling gas	25	60
HT to the main cooling gas	50	15
HTO to the vented gas	5	17
HT to the vented gas	20	5

The consequence is that tritium can be removed from the circuit by operating at higher moisture levels and by absorbing moisture in a molecular sieve in a bypass, e.g., the fission gas cleanup system. The moisture must be removed to protect the LN-cooled charcoal filter in the cleanup system. At lower H₂ and H₂O levels, a copper oxide bed must be employed to convert HT to HTO, but it is very unlikely that levels lower than 90 and 30 vpm, respectively, will be employed in a GCFR.

5.2. Iodine

Iodine measurements have been made. In spite of a very sensitive measuring device no iodine could be detected. The iodine is probably trapped in the hot active charcoal filters in the bundle, as expected.

6. FUTURE EXPERIMENTAL WORK

The initial objective of the HELM 3 test is to reach a burnup of 60 MWd/kg, because Cs deposition seems to become significant at 40 MWd/kg and may hinder the fission gas venting. Whether the irradiation is continued to 100 MWd/kg has not yet been decided. A bundle with a cladding leak in one rod (HELM 4) is being considered. Besides that, three single rod experiments similar to GB-10 (see Part 1) are under preparation and are planned to be irradiated by the end of 1980.

REFERENCES

H. Euringer, W. Krauthausen, and W. Krug, "Dummy Test Facility (DTF)," Bericht 3, Betrieb, Auswertung Ergebnisse, Interner Bericht, KFA-ZBB-B-11/76, September 1976.

M. Dalle Donne, et al., "BR2 Bundle Mockup Heat Transfer Experiments and Calculations," NEA - Specialist Meeting, Mol, April 18-19, 1978.

W. Jung, "GCFR Test Fuel Element Design," NEA - Specialist Meeting, Mol, April 18-19, 1978.

H. Euringer, et al., "GSB - Brennelement Bestrahlungen im He-Loop Mol," 25th Meeting of Irradiation Devices Working Group in Petten, May 18-19, 1978.